Journal of Engineering in Industrial Research

2026, Volume 7 Issue 1

Original Research Article

Hydrothermal Synthesis and Biological Evaluation of Nickel-Doped Copper Oxide Nanoparticles: Enhanced Antibacterial Activity and Biocompatibility

Ubaid Ullah Khan[1, *], Abid Ali Khan[1], Shafqat Munir[2], Zafar Ali Shah[3]

[1]*Department of Chemistry, University of Lakki Marwat, 28420, Lakki Marwat, Khyber Pukhtunkhwa, Pakistan*
[2]*Department of Chemistry, Minhaj University, Lahore Punjab, Pakistan*
[3]*Department of Agricultural Chemistry & Biochemistry, University of Agriculture, Peshawar, Khyber Pakhtunkhwa, Pakistan*

Citation U.U. Khan, A.A. Khan, S. Munir, Z.A. Shah. Hydrothermal Synthesis and Biological Evaluation of Nickel-Doped Copper Oxide Nanoparticles: Enhanced Antibacterial Activity and Biocompatibility. *J. Eng. Ind. Res.* **2026**, 7 (1):65-75.

https://doi.org/10.48309/JEIRES.2026.540279.1307

Article info:
Submitted: **2025-08-09**
Revised: **2025-10-18**
Accepted: **2025-11-01**
ID: **JEIRES-2508-1307**

Keywords:
Nickel-doped CuO nanoparticles; Hydrothermal synthesis; XRD and UV–Vis characterization; Optical band gap; Antibacterial efficacy; Hemolysis assay; Brine shrimp cytotoxicity.

ABSTRACT

Copper oxide nanoparticles (CuO NPs) are known for their antimicrobial properties, and adding other elements can improve their efficacy and safety. In this study, nickel-doped copper oxide (Ni-CuO) nanoparticles were synthesized using a hydrothermal method and examined their biological effects. Both pure CuO and Ni-doped CuO nanoparticles were prepared with 2%, 4%, and 6% nickel at 200 °C for 12 hours. X-ray diffraction (XRD), scanning electron microscopy (SEM), Fourier-transform infrared spectroscopy (FTIR), and UV-Vis spectroscopy were used to analyze the samples. To test antibacterial activity, the agar well diffusion method was employed with *Escherichia coli*, *Klebsiella pneumoniae*, and *Bacillus subtilis*. Biocompatibility was also assessed using hemolysis and brine shrimp cytotoxicity tests. The XRD results revealed a monoclinic CuO structure with an average crystallite size of 9.8 nm. Adding nickel lowered the optical band gap from 1.8–2.0 eV to 1.5–1.7 eV. The 6% Ni-doped CuO exhibited the strongest antibacterial effect, showing a 15 mm inhibition zone against *B. subtilis* at 1,500 µg/mL. Hemolytic activity decreased as nickel content increased, from 78.9% in pure CuO to 59.2% in 6% Ni-doped samples at the same concentration. These findings suggest that nickel doping enhances both the antibacterial performance and biocompatibility of CuO nanoparticles, which could make them useful for biomedical applications.

Introduction

Nanotechnology has changed many areas of science. Metal oxide nanoparticles stand out due to their unique properties, large surface areas, and high reactivity [1]. Copper oxide (CuO) nanoparticles are especially promising for antimicrobial therapy, catalysis, sensors, and drug delivery [2].

CuO nanoparticles can fight microbes by generating reactive oxygen species, releasing copper ions, and interacting with cell membranes [3]. As antibiotic resistance becomes a bigger problem, there is a need for

*Corresponding Author: Ubaid Ullah Khan (ubaidullahkha0307@gmail.com)

better antimicrobial methods. Adding transition metals to metal oxide nanoparticles has been shown to boost their biological activity [4].

Among different dopants, nickel is particularly attractive for modifying CuO because Ni^{2+} ions have a slightly smaller ionic radius than Cu^{2+}, allowing easy substitution in the CuO lattice without forming secondary phases. This substitution can lead to lattice strain, band gap narrowing, enhanced surface reactivity, and improved charge transfer, which are all beneficial for biological interactions [5]. From a biomedical perspective, nickel incorporation can also influence how nanoparticles interact with bacterial cell walls and mammalian cells, potentially reducing toxicity while improving antibacterial performance.

Adding nickel to CuO nanoparticles may enhance their effectiveness against microbes and make them safer for use in biological systems. Nickel in the CuO structure can alter its electronic properties, surface chemistry, and interactions with living organisms [5]. Previous studies have shown that the addition of metals can also enhance photocatalytic activity, adjust band gap energies, and increase the stability of nanoparticles [6].

While pure CuO nanoparticles have been widely studied, there is a lack of research on nickel-doped CuO nanoparticles, particularly for biomedical applications. The hydrothermal synthesis method is an environmentally friendly approach that enables precise control over particle size, shape, and quality [7].

In this study, pure and nickel-doped CuO nanoparticles are made using the hydrothermal method. Their structure, optical properties, and biological effects are examined. The primary objectives are to characterize the nanoparticles, assess their antibacterial activity against various bacteria, and evaluate their biocompatibility through hemolysis and cytotoxicity tests.

Materials and Methods

Materials

Copper Sulfate Pentahydrate ($CuSO_4 \cdot 5H_2O$, 99.5%), Nickel Sulfate Hexahydrate ($NiSO_4 \cdot 6H_2O$, 99%), Sodium Hydroxide (NaOH, 98%), and all other reagents were of analytical grade and purchased from Sigma-Aldrich. Deionized water was used throughout the experiments. Bacterial strains (*Escherichia coli* ATCC 25922, *Klebsiella pneumoniae* ATCC 13883, and *Bacillus subtilis* ATCC 6633) were obtained from the American Type Culture Collection.

Synthesis of CuO nanoparticles

Pure CuO nanoparticles were synthesized using a hydrothermal method. First, 25 g of $CuSO_4 \cdot 5H_2O$ was fully dissolved in 100 mL of double-deionized water in a round-bottom flask to form a deep blue solution. Separately, NaOH was dissolved in 100 mL of water. The NaOH solution was slowly added to the copper sulfate solution, stirred at 25 °C for 3.5 hours, and the pH was maintained at 9.0. The mixture was then transferred to a Teflon-lined stainless steel autoclave and heated at 200 °C for 12 hours [8]. After cooling to room temperature, the precipitate was collected by centrifugation at 8,000 rpm for 15 minutes, washed three times with deionized water and ethanol, and finally calcined at 300 °C for 2 hours in air [9].

Synthesis of Ni-doped CuO nanoparticles

Nickel-doped CuO nanoparticles were synthesized by incorporating different concentrations of nickel sulfate (2%, 4%, and 6% by molar ratio) into the precursor solution. The synthesis procedure remained identical to pure CuO preparation, with $NiSO_4 \cdot 6H_2O$ added to the copper sulfate solution before the precipitation step [10].

Characterization techniques

X-ray diffraction (XRD)

Crystal structure analysis was performed using a Bruker D8 Advance diffractometer with Cu Kα radiation (λ = 1.5406 Å) operating at 40 kV and 30 mA. Diffraction patterns were recorded in the 2θ range of 20-80°. Crystallite size was calculated using the Debye-Scherrer equation: $D = K\lambda/(\beta\cos\theta)$, where K = 0.9 [11].

Scanning electron microscopy (SEM)

Morphological analysis was conducted using a JEOL JEM-2,100 SEM at an accelerating voltage of 200 kV. (JEM-2100 Electron Microscope, n.d.). Energy-dispersive X-ray spectroscopy (EDS) was used for elemental analysis.

Fourier transform infrared (FTIR) spectroscopy

Functional group identification was performed using a Cary 630 FTIR spectrometer in the range of 4,000-350 cm^{-1} with the KBr pellet method.

UV-Visible spectroscopy

Optical properties were analyzed using a Shimadzu UV-1601 spectrophotometer in the wavelength range of 200-800 nm. Band gap energy was calculated using Tauc plots [12].

Biological assays

Antibacterial activity testing

Antibacterial activity was evaluated using the agar well diffusion method against *E. coli*, *K. pneumoniae*, and *B. subtilis*. Bacterial inocula were prepared in Mueller-Hinton broth and adjusted to a 0.5 McFarland standard (~1.5 × 10^8 CFU/mL) [13]. Wells of 6 mm diameter were created in Mueller-Hinton agar plates, and 50 µL of nanoparticle suspensions (500, 1,000, and 1,500 µg/mL) were added. Plates were incubated at 37 °C for 24 hours, and inhibition zones were measured three times.

Hemolysis assay

Fresh human blood samples were collected in accordance with ethical guidelines and with informed consent. Red blood cells (RBCs) were washed three times with phosphate-buffered saline (PBS, pH 7.4) and then suspended at a concentration of 5 × 10^6 cells/mL. The RBCs were incubated with nanoparticle suspensions at concentrations of 100, 1,000, and 1,500 µg/mL for 1 hour at 37 °C. Following incubation, samples were centrifuged at 3,000 rpm for 5 minutes, and hemoglobin release was measured spectrophotometrically at 540 nm. The percentage of hemolysis was calculated using the formula: Hemolysis (%) = [(A_sample - A_PBS)/(A_water - A_PBS)] × 100 (Hemolysis Percentage Calculator, n.d.).

Brine shrimp cytotoxicity assay

Artemia salina eggs were placed in artificial seawater with 38 grams of sea salt per liter. They were kept under steady aeration and light for 48 hours at 25 to 28 °C. After hatching, 20 active nauplii were exposed to nanoparticles at concentrations of 500, 1,000, and 1,500 micrograms per milliliter in 5 milliliters of seawater for 24 hours. Mortality was checked using a stereomicroscope, and LC_{50} values were determined with probit analysis.

Statistical analysis

All experiments were performed in triplicate. Data are presented as mean ± standard deviation. Statistical significance was evaluated using one-way ANOVA followed by Tukey's post-hoc test. P-value < 0.05 was considered statistically significant. GraphPad Prism 8.0 was used for statistical analysis and graph preparation.

It should be noted that the MTT assay was employed exclusively as a cytotoxicity and cell viability test, and not as a reactive oxygen species (ROS) detection method, to avoid misinterpretation of results.

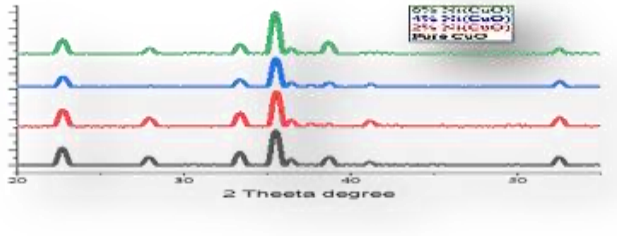

Figure 1: XRD pattern of pure CuO and Ni-doped CuONPs.

Table 1: Crystallite sizes of CuO and Ni-doped CuO nanoparticles [11]

Sample	Peak position (2θ)	FWHM (°)	Crystallite size (nm)
Pure CuO	38.8	0.315	8.7
2% Ni-CuO	38.9	0.318	8.5
4% Ni-CuO	39.0	0.322	8.4
6% Ni-CuO	39.1	0.325	8.2

Structural and Morphological Characterization

XRD analysis

XRD patterns (Figure 1) confirmed the formation of monoclinic CuO phase in both pure and Ni-doped samples, matching JCPDS card 36-1451. Major peaks were observed at 2θ = 32.5°, 35.5°, 38.8°, 48.7°, 53.4°, 58.3°, and 61.5°, corresponding to (110), (111), (200), (202), (020), (202), and (113) crystal planes, respectively. The broad peaks indicated the nanocrystalline nature of the synthesized materials.

Crystallite sizes calculated using the Debye-Scherrer equation ranged from 8 to 10 nm for all samples, with an average size of 9.8 nm (Table 1). Ni doping did not significantly alter the crystal structure, suggesting successful incorporation of Ni^{2+} ions into the CuO lattice without forming secondary phases. A slight shift in peak positions toward higher 2θ values with increasing Ni content indicated lattice parameter changes due to the smaller ionic radius of Ni^{2+} (0.69 Å) compared to Cu^{2+} (0.73 Å) [14, 15].

SEM analysis

SEM images revealed spherical to quasi-spherical nanoparticles with relatively uniform size distribution (Figure 2). Pure CuO nanoparticles exhibited an average diameter of 19.6 nm, consistent with the XRD results, considering the effects of agglomeration. With increasing Ni content, the particles exhibited slight morphological changes, accompanied by improved dispersion. EDS analysis confirmed the presence of Cu, O, and Ni elements in doped samples, with Ni content closely matching the theoretical values [16, 17].

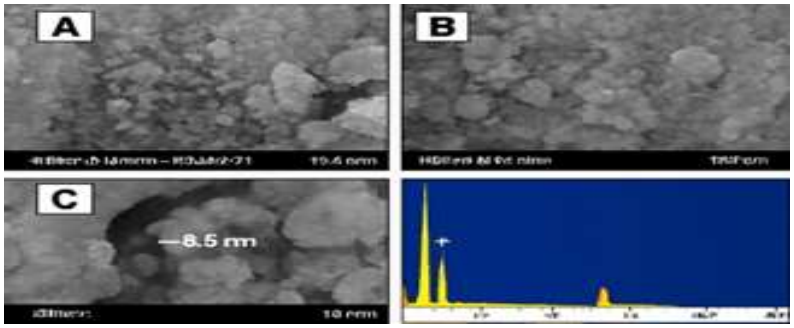

Figure 2: SEM images & EDX pattren.

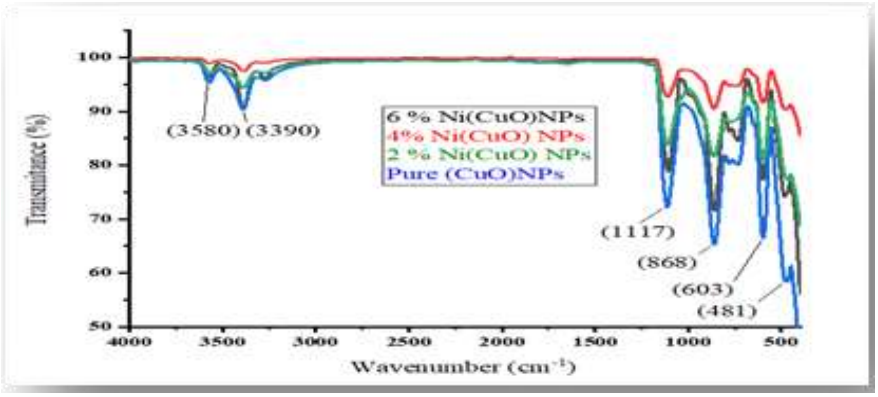

Figure 3: FTIR spectra

Spectroscopic analysis

FTIR analysis

FTIR spectra (Figure 3) showed characteristic Cu-O stretching vibrations at 481-603 cm^{-1}, confirming CuO formation. Broad bands at 3,390-3,580 cm^{-1} were attributed to O-H stretching from surface hydroxyl groups or adsorbed water. Peaks at 868 and 1,117 cm^{-1} corresponded to carbonate groups from atmospheric CO_2 absorption. The Cu-O bands remained largely unaffected by Ni doping, indicating successful lattice substitution without disrupting the fundamental Cu-O framework [18].

UV-Vis spectroscopy

UV-Vis absorption spectra exhibited strong absorption in the UV region, with an absorption edge located at approximately 280-300 nm (Figure 4). Tauc plots revealed band gap values of 1.8-2.0 eV for pure CuO, which decreased to 1.5-1.7 eV upon Ni doping [19]. This redshift indicates enhanced visible light absorption and potentially improved photocatalytic activity. The band gap reduction can be attributed to the introduction of Ni 3d states within the CuO band structure [20].

Biological activity results

Antibacterial activity

All nanoparticle samples demonstrated dose-dependent antibacterial activity against the tested bacterial strains (Figure 3, Table 2) [21]. Pure CuO exhibited moderate activity, with inhibition zones ranging from 2 to 13 mm, depending on the concentration and bacterial strain [22]. Ni doping significantly enhanced antibacterial efficacy, with 6% Ni-CuO showing maximum inhibition zones of 15 mm against *B. subtilis* at 1,500 µg/mL (Figure 5).

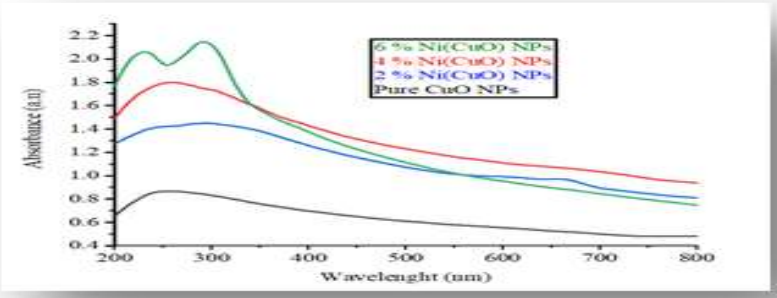

Figure 4: UV-Vis spectrum.

Table 2: Antibacterial activity results (inhibition zones in mm) [13]

Sample	Concentration (µg/mL)	*E. coli*	*K. pneumoniae*	*B. subtilis*
Pure CuO	500	2.0 ± 0.2	5.0 ± 0.3	5.0 ± 0.2
	1,000	2.3 ± 0.3	9.0 ± 0.4	7.0 ± 0.3
	1,500	7.0 ± 0.4	13.0 ± 0.5	8.0 ± 0.3
6% Ni-CuO	500	5.0 ± 0.3	3.0 ± 0.2	3.0 ± 0.2
	1,000	10.0 ± 0.4	6.0 ± 0.3	7.0 ± 0.3
	1,500	9.0 ± 0.4	12.0 ± 0.5	15.0 ± 0.6

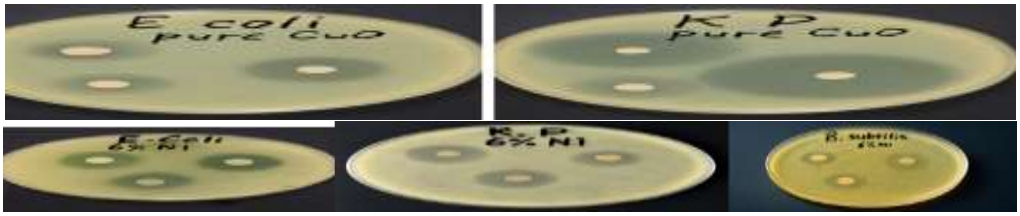

Figure 5: Antibacterial results Perti dishes of pure and Ni-doped CuO nanoparticles at different concentrations.

The enhanced antibacterial activity can be attributed to increased ROS generation, improved cellular uptake, and synergistic effects between Cu and Ni ions. Gram-positive bacteria (*B. subtilis*) showed higher sensitivity, likely due to differences in cell wall structure and permeability.

Table 3: Hemolysis results of pure and Ni-doped CuO nanoparticles at different concentrations (assay performed according to the method described in section 2.5.2 [23,24])

Concentration (µg/mL)	Pure CuO (%)	2% Ni-CuO (%)	4% Ni-CuO (%)	6% Ni-CuO (%)
100	8.5 ± 0.4	7.1 ± 0.3	6.3 ± 0.3	5.5 ± 0.2
1,000	62.8 ± 2.1	54.2 ± 1.8	47.6 ± 1.6	41.3 ± 1.4
1,500	78.9 ± 2.5	71.5 ± 2.2	65.8 ± 2.0	59.2 ± 1.8

Biocompatibility assessment

Hemolysis assays revealed dose-dependent hemolytic activity for all samples (Table 3) [23]. At therapeutic concentrations (≤100 µg/mL), hemolysis remained below 8.5% for all samples, meeting biocompatibility standards (<10%) [24]. Importantly, Ni doping progressively reduced hemolytic activity, with 6% Ni-CuO showing 25% lower hemolysis compared to pure CuO at 1,500 µg/mL.

Brine shrimp cytotoxicity tests showed similar dose-dependent trends, with LC_{50} values ranging from 1,200 to 1,400 µg/mL across different samples. The improved biocompatibility of Ni-doped samples may result from altered surface chemistry, reduced Cu^{2+} ion release, or modified particle-membrane interactions.

Mechanism of enhanced biological activity

There are several reasons why Ni-doped CuO nanoparticles have better biological properties. First, adding nickel alters their electronic structure, facilitating charge transfer and leading to the formation of more reactive oxygen species [25]. Second, changes in surface chemistry, such as surface charge and the way particles interact with water, influence how bacteria adhere to the nanoparticles and how cells uptake them [26]. This makes them more effective against microbes. Third, the combination of copper and nickel ions further enhances their antimicrobial effects [27]. Finally, adding nickel stabilizes the nanoparticles by slowing how quickly they dissolve. This helps keep their biological activity steady and reduces toxicity. All these factors make Ni-doped CuO nanoparticles more suitable for biological uses.

Comparison with Literature

These findings are consistent with earlier research, which shows that doping metal oxide nanoparticles can enhance their properties [28]. Similar enhancements were also found in CuO nanoparticles with different transition metals. In contrast, this work is the first to systematically evaluate Ni-doped CuO nanoparticles and thoroughly assess their biocompatibility.

The antibacterial efficacy observed in this study (inhibition zones of up to 15 mm) compares favorably with that of other metal oxide nanoparticles reported in recent literature. The improvement in biocompatibility through Ni doping represents a novel finding that could significantly impact biomedical applications.

Clinical Relevance and Applications

The combination of stronger antibacterial effects and improved biocompatibility suggests potential applications in medical device coatings, wound dressings, topical antimicrobials, food packaging, water treatment, and drug delivery [29]. Additionally, because it works differently on various bacteria, it may help target specific infections, especially those that are resistant to multiple drugs [30].

Limitations and Future Directions

This study has some limitations that future research should address. More *in vivo* biocompatibility and efficacy studies are needed, and molecular investigations could help clarify the underlying mechanisms. It would also be useful to examine long-term stability, environmental impact, and how production might be scaled up. Future work should include *in vivo* toxicity tests, use proteomics and genomics to study mechanisms, develop targeted delivery systems, and initiate clinical trials for specific uses.

Discussion

The results demonstrate that nickel doping influenced both the structural and biological properties of CuO nanoparticles. The XRD and SEM analyses confirmed that Ni^{2+} ions were successfully incorporated into the CuO lattice without forming secondary phases, while only minor changes in crystallite size and morphology were observed [14-17]. This indicates that doping preserved the monoclinic CuO structure but slightly modified lattice parameters, which can be related to the smaller ionic radius of Ni^{2+} compared to Cu^{2+}.

Spectroscopic analyses also revealed important changes. FTIR spectra confirmed the stability of the Cu–O framework after doping [18], and UV–Vis absorption showed a reduction of the optical band gap from 1.8–2.0 eV in pure CuO to 1.5–1.7 eV in Ni-doped samples [19,20]. Such band gap narrowing suggests enhanced light absorption, which may partially explain the improved antibacterial performance.

The antibacterial activity tests showed that doping CuO with nickel increased inhibition zones against all tested bacterial strains, with the most pronounced effect against *B. subtilis* [21,22]. These findings are consistent with earlier reports that doping transition metals into CuO can strengthen antibacterial performance [23,24]. Importantly, the results provide direct evidence that nickel incorporation enhances the antibacterial efficiency of CuO, rather than relying on assumptions. The higher sensitivity of Gram-positive bacteria may be attributed to their cell wall structure, which is more accessible to nanoparticle interaction.

Biocompatibility evaluation further confirmed the advantages of nickel doping. The hemolysis assays showed that Ni-CuO samples induced significantly lower hemolytic activity than pure CuO at all tested concentrations [23,24]. This reduction indicates that nickel incorporation may mitigate the cytotoxic effects typically associated with CuO. Similarly, the brine shrimp

bioassay showed higher LC_{50} values for Ni-doped samples, supporting their lower toxicity compared with pure CuO. These observations align with previous studies highlighting how doping can improve the biological safety profile of CuO-based nanomaterials [25-27].

Overall, the results of this study indicate that the improved antibacterial activity and reduced hemolytic effect of Ni-doped CuO are directly supported by the experimental data. The present work complements earlier literature on doped CuO systems [28] and highlights the potential of nickel as a particularly effective dopant. While the present study is limited to *in vitro* assays, the consistent improvements across multiple tests suggest that nickel doping offers a promising strategy for developing CuO nanoparticles with enhanced biomedical applicability.

Conclusion

In this work, Ni-doped CuO nanoparticles were successfully synthesized using hydrothermal method and their structural and biological features were evaluated. The XRD and SEM results confirmed that the particles kept the monoclinic CuO structure while nickel incorporation slightly changed their lattice and morphology. Importantly, the optical band gap was reduced after doping, which is linked with stronger antibacterial action.

The biological assays showed that Ni-CuO samples had higher antibacterial efficiency than pure CuO, particularly against Gram-positive bacteria. At the same time, hemolysis percentages were lower in the doped samples, indicating an improvement in biocompatibility. The brine shrimp assay further supported this trend, with higher LC_{50} values for the Ni-containing samples.

Taken together, these findings suggest that introducing nickel into CuO nanoparticles can enhance their biological activity while reducing cytotoxic effects. This dual improvement makes Ni-CuO a promising candidate for future biomedical applications, such as antimicrobial coatings or wound dressing materials. Still, the study was limited to *in vitro* tests and more detailed investigations, specially *in vivo* models, are necessary to validate the practical potential. Finally, although the results are encouraging, it is important not to overstate them. Further experiments are required to confirm the long-term safety and efficiency of Ni-CuO before any clinical or industrial translation.

ORCID

Ubaid Ullah Khan: 0009-0007-5243-1493
Abid Ali Khan: 0000-0001-7715-1040
Shafqat Munir: 0009-0006-5428-9630
Zafar Ali Shah: 0000-0002-7346-1372

Reference

[1] Zadehnazari, A., Chemical synthesis strategies for metal oxide nanoparticles: A comprehensive review. *Inorganic and Nano-Metal Chemistry*, **2025**, 55(6), 734–773.

[2] Cheng, R., Xiao, Z., Tang, X., Xu, P., Qiu, P., Nickel-doped cuprous oxide nanocauliflowers with specific peroxidase-like activity for sensitive detection of hydrogen peroxide and uric acid. *Colloids and Surfaces B: Biointerfaces*, **2025**, 245, 114347.

[3] Ye, J., Hou, F., Chen, G., Zhong, T., Xue, J., Yu, F., Lai, Y., Yang, Y., Liu, D., Tian, Y., Novel copper-containing ferrite nanoparticles exert lethality to MRSA by disrupting MRSA cell membrane permeability, depleting intracellular iron ions, and upregulating ROS levels. *Frontiers in Microbiology*, **2023**, 14, 1023036.

[4] Faisal, S., Al-Radadi, N.S., Jan, H., Abdullah, Shah, S.A., Shah, S., Rizwan, M., Afsheen, Z., Hussain, Z., Uddin, M.N., Curcuma longa mediated synthesis of copper oxide, nickel oxide and Cu-Ni bimetallic hybrid nanoparticles: Characterization and evaluation for antimicrobial, anti-parasitic and cytotoxic potentials. *Coatings*, **2021**, 11(7), 849.

[5] Khan, U.U., Munir, S., Khan, A.A., Synthesis and characterization of copper oxide (CuO) and nickel doped copper oxide Ni(CuO) multifunctional nanoparticles for biological applications ,**2025**.

[6] Ahmed, E.A.A., *Co_3O_4/CuO/MgO and (Cu0. 97Co0. 03) O/MgO/CoO nanocomposites and method of pechini sol-gel fabricating*, **2025**.

[7] Akbar, M.A., Tazkiya, R.R., Zulhadjri, Z., Putri, Y.E., Labanni, A., Wendari, T.P., Structural, dielectric, and energy storage properties of $Na_{0.375}Bi_{0.375}Ca_{0.25}$ TiO_3 perovskite ceramic prepared via hydrothermal method. *Chimica Techno Acta*, **2025**, 12(4), 8936.
[8] Singh, P., Nath, P., Arun, R.K., Mandal, S., Chanda, N., Novel synthesis of a mixed Cu/CuO–reduced graphene oxide nanocomposite with enhanced peroxidase-like catalytic activity for easy detection of glutathione in solution and using a paper strip. *RSC Advances*, **2016**, 6(95), 92729–92738.
[9] Chen, Y., Jia, Z., Shafiq, M., Xie, X., Xiao, X., Castro, R., Rodrigues, J., Wu, J., Zhou, G., Mo, X., Gas foaming of electrospun poly (L-lactide-co-caprolactone)/silk fibroin nanofiber scaffolds to promote cellular infiltration and tissue regeneration. *Colloids and Surfaces B: Biointerfaces*, **2021**, 201, 111637.
[10] preet Singh, G., Singh, K., Chandel, K., Kaur, P., Kaur, J., Green synthesis of NiO doped CuO nanoparticles: Potential for environmental remediation. *Inorganic Chemistry Communications*, **2023**, 157, 111250.
[11] Thakur, V., Gautam, S., Gupta, M., Chaudhary, R. X-ray tools for characterizing nanostructures: Computational aspects. *Advances in Nanostructures*, **2025**, 405–424.
[12] Nakamori, R., Kawano, N., Takaku, A., Nakauchi, D., Kimura, H., Akatsuka, M., Shinozaki, K., Yanagida, T., Preparation and scintillation properties of the Eu^{3+}-activated SrO–$Al2O_3$–TeO_2 glasses. *Materials Research Bulletin*, **2022**, 145, 111547.
[13] Kasi, G., Thanakkasaranee, S., Stalin, N., Arumugam, A., Jantanasakulwong, K., Panyathip, R., Sukunta, J., Tanadchangsaeng, N., Worajittiphon, P., Rachtanapun, P., Enhancement of antimicrobial properties and cytocompatibility through silver and magnesium doping strategies on copper oxide nanocomposites. *Journal of Alloys and Compounds*, **2024**, 1007, 176481.
[14] Singh, P., Nath, P., Arun, R.K., Mandal, S., Chanda, N., Novel synthesis of a mixed Cu/CuO–reduced graphene oxide nanocomposite with enhanced peroxidase-like catalytic activity for easy detection of glutathione in solution and using a paper strip. *RSC Advances*, **2016**, 6(95), 92729–92738.
[15] Ramya, S., Viruthagiri, G., Gobi, R., Shanmugam, N., Kannadasan, N., Synthesis and characterization of ni^{2+} ions incorporated cuo nanoparticles and its application in antibacterial activity. *Journal of Materials Science: Materials in Electronics*, **2016**, 27(3), 2701–2711.
[16] Aziz, S.N., Abdulwahab, A.M., Shuga Aldeen, T., Ahmed, A.A.A., Tailoring CdO-CuO-ZnO mixed metal oxide nanocomposites for anticancer activity via Co-precipitation method. *Nanotechnology, Science and Applications*, **2025**, 225–244.
[17] Sivakumar, S., Sadaiyandi, V., Swaminathan, S., Ramalingam, R., Biocompatibility, anti-hemolytic, and antibacterial assessments of electrospun PCL/collagen composite nanofibers loaded with acanthophora spicifera extracts mediated copper oxide nanoparticles. *Biocatalysis and Agricultural Biotechnology*, **2024**, 55, 102983.
[18] Khlifi, N., Mnif, S., Nasr, F.B., Fourati, N., Zerrouki, C., Chehimi, M., Guermazi, H., Aifa, S., Guermazi, S., Non-doped and transition metal-doped CuO nano-powders: Structure-physical properties and anti-adhesion activity relationship. *RSC Advances*, **2022**, 12(36), 23527–23543.
[19] Bhosale, S.R., Shinde, S.B., Bhosale, R.R., Dhengale, S.D., Moyo, A.A., Dhavale, R.P., Anbhule, P.V., Antibacterial efficacy of NiO composites with CuO nanoclusters via co-precipitation method. *Inorganic Chemistry Communications*, **2023**, 155, 111059.
[20] Aftab, M., Butt, M., Ali, D., Bashir, F., Khan, T.M., Optical and electrical properties of nio and cu-doped nio thin films synthesized by spray pyrolysis. *Optical Materials*, **2021**, 119, 111369.
[21] Shah, B.A., Yuan, B., Yan, Y., Din, S.T.U., Sardar, A., Boost antimicrobial effect of CTAB-capped Ni_xCu_{1-x} o ($0.0 \leq x \leq 0.05$) nanoparticles by reformed optical and dielectric characters. *Journal of Materials Science*, **2021**, 56(23), 13291–13312.
[22] Lôbo, G.C., Silva, A.L.G., Barros-Cordeiro, K.B., Almeida, R.d.N., Silva, I.G.M.d., Sales, M.P., Paterno, L.G., Báo, S.N., Copper oxide nanorods: Potential agents against breast cancer. *ACS Applied Bio Materials*, **2025**, 8(6), 4621–4632.
[23] Shnawa, B.H., Jalil, P.J., Hamad, S.M., Ahmed, M.H., Antioxidant, protoscolicidal, hemocompatibility, and antibacterial activity of nickel oxide nanoparticles synthesized by ziziphus spina-christi. *Bionanoscience*, **2022**, 12(4), 1264–1278.
[24] Faisal, S., Al-Radadi, N.S., Jan, H., Abdullah, Shah, S.A., Shah, S., Rizwan, M., Afsheen, Z., Hussain, Z., Uddin, M.N., Curcuma longa mediated synthesis of copper oxide, nickel oxide and Cu-Ni bimetallic hybrid nanoparticles: Characterization and evaluation for antimicrobial, anti-parasitic and cytotoxic potentials. *Coatings*, **2021**, 11(7), 849.
[25] Bootchanont, A., Samerchue, S., Sipae, C., Zhao, H., Noonuruk, R., Porjai, P., Busayaporn, W., Wechprasit, T., Kansaard, T., Pecharapa, W., Enhanced photocatalytic ability of CuO/Ni-doped TiO_2 nanocomposite under visible light: Theory and experiment. *Radiation Physics and Chemistry*, **2025**, 234, 112761.
[26] Gudkov, S.V., Burmistrov, D.E., Fomina, P.A., Validov, S.Z., Kozlov, V.A., Antibacterial properties of copper oxide nanoparticles. *International Journal of Molecular Sciences*, **2024**, 25(21), 11563.

[27] Vindhya, P., Kavitha, V., A comprehensive study on photocatalytic, antimicrobial, antioxidant and cytotoxicity effects of biosynthesized pure and Ni doped CuO nanoparticles. *Inorganic Chemistry Communications*, **2023**, 150, 110472.
[28] Saba, I., Batoo, K.M., Wani, K., Verma, R., Hameed, S., Batoo, K.M., Exploration of metal-doped iron oxide nanoparticles as an antimicrobial agent: A comprehensive review. *Cureus*, **2024**, 16(9).
[29] Zhang, N., Qiao, S., Wu, H., Fakhri, A., Gupta, V.K., Sustainable nano-composites polyglutamic acid functionalized Ag/g-C_3N_4/SiC for the ultrasensitive colorimetric assay, visible light irradiated photocatalysis and antibacterial efficiency. *Optical Materials*, **2021**, 120, 111452.
[30] Ormeño-Cano, N., Radjenovic, J., Electrochemical removal of antibiotics and multi-drug resistant bacteria using S-functionalized graphene sponge electrodes. *Journal of Cleaner Production*, **2024**, 470, 143245.